PCCP

Accepted Manuscript

ROYAL SOCIETY OF CHEMISTRY

www.rsc.org/pccp

Physical Chemistry Chemical Physics
CREATED USING THE RSC LaTeX PCCP ARTICLE TEMPLATE – SEE www.rsc.org/electronicfiles FOR DETAILS
ARTICLE TYPE www. rsc.org/xxxxxx | XXXXXXXX

How disorder controls the kinetics of triplet charge recombination in semiconducting organic polymer photovoltaics

Eric R. Bittner*[a], Vladimir Lankevich[a], Simon Gélinas[b], Akshay Rao[b], David A. Ginger[c], and Richard H. Friend[b]

Received Xth XXXXXXXXXX 20XX, Accepted Xth XXXXXXXXX 20XX
First published on the web Xth XXXXXXXXXX 200X
DOI: 10.1039/b000000x

Recent experiments by Rao *et al.* (Nature, 2013 **500**, 435-439) indicate that recombination of triplet charge-separated states is suppressed in organic polymer/fullerene based bulk-heterojunction (BHJ) photovoltaic cells exhibiting a high degree of crystallinity in the fullerene phase relative to systems with more disorder. In this paper, we use a series of Frenkel-exciton lattice models to rationalize these results in terms of wave-function localization, interface geometry, and density of states. In one-dimensional co-linear and co-facial models of the interface, increasing local energetic disorder in one phase localizes the interfacial triplet charge-transfer (^{3}CT) states and increases the rate at which these states relax to form lower-energy triplet excitons. In two dimensional BHJ models, energetic disorder within the fullerene phase plays little role in further localizing states pinned to the interface. However, inhomogeneous broadening introduces strong coupling between the interfacial ^{3}CT and nearby fullerene triplet excitons and can enhance the decay of these states in systems with higher degrees of energetic disorder.

1 Introduction

Photovoltaic diodes based on blends of semiconductor polymers and fullerene derivatives now produce power conversion efficiencies exceeding 10% under standard solar illumination[1]. This indicates that photocarriers can be generated efficiently in well-optimized organic heterostructures. However, the photo physical pathways for converting highly-bound Frenkel excitons to photocarriers are poorly understood in spite of vigorous, multidisciplinary research activity.

A detailed understanding of primary charge generation dynamics is of key fundamental importance in the development of organic solar cells.[2] Fig. 1 provides a summary of the important relaxation pathways. Singlet Frenkel excitations are created within the bulk of cell by photo excitation of the singlet ground state. Vibronic coupling leads to self-trapped excitons that are localized to at most a few molecular units (1). Within a bulk heterojunction system, the energetic offset between donor and acceptor materials provides the driving force for charge separation. Singlet excitons (S_1) created by photo excitation in the bulk dissociate to form either charge-separated (CS) states (2) and polarons or interfacial charge-transfer state pinned by their mutual Coulombic attraction to the phase boundary between donor and acceptor domains (3). These exciplex states do carry some oscillator strength to the singlet S_o ground state and can decay radiatively on the time scale of nanoseconds.

In order to produce current, the electron and hole must overcome their mutual Coulombic attraction and be separated at a distance $R > 2e^2/(3\varepsilon k_B T)$, assuming a homogeneous 3D medium with dielectric constant ε. For typical organic systems with $\varepsilon = 2$ to 3, charges must be separated by about 100Å in order to be considered "free" carriers, P^+ and P^-. Recent spectroscopic measurements on organic photovoltaic (OPV) systems have reported that photoexcited charges can be generated on $\leq$ 100-fs timescales[3–10] but full charge separation to produce photocarriers was expected to be energetically expensive given strong Coulombic barriers due to the low dielectric constant in molecular semiconductors. Nonetheless, experiments by Gélinas *et al.*, in which Stark effect signatures in transient absorption spectra were analyzed to probe the local electric field as charge separation proceeds, indicate that electrons and holes separate by $\sim$40 Å over the first 100 fs and evolve further on picosecond timescales to produce unbound charge pairs[11]. The short-time dynamics reported in Refs. 11,12 indicate that coherent processes play an important role in the direct production of mobile charge carriers in OPV systems[13].

[a] *Department of Chemistry, University of Houston, 4800 Calhoun St., Houston TX, USA. Fax: 01 713-743-2709; Tel: 01 832-316-8849; E-mail: bittner@uh.edu*
[b] *Cavendish laboratory, University of Cambridge, JJ Thomson Avenue, Cambridge CB30HE, UK.*
[c] *Department of Chemistry, University of Washington, Seattle, Washington 98195-1700, USA.*
ERB and VL performed the calculations and analyzed the numerical data. Data and results were shared with all authors over the course of the work. ERB supervised the work and wrote the manuscript. All authors commented on the manuscript. Correspondence should be addressed to ERB (bittner@uh.edu).

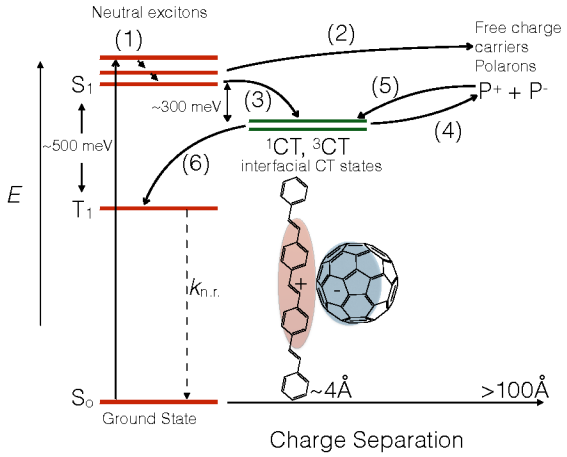

Fig. 1 Photophysical pathways for charge-carrier generation in an organic photovoltaic cell.

At sufficiently high carrier densities, bimolecular encounters between non-geminate and uncorrelated polaron pairs, P^+P^-, can form either singlet or triplet CT states (5)

$$P^+ + P^- \rightleftharpoons {}^3\text{CT or } {}^1\text{CT}$$

with a 3:1 branching ratio dictated by spin-statistics. Generally speaking, the energy difference between singlets and triplets is twice the exchange interaction. and one can assume that charge separated states such as ^{1}CT and ^{3}CT are nearly energetically degenerate and can re-dissociate (4) back into polaron pairs. The triplet excitons, T_1, are about 0.4eV lower in energy than S_1 singlet excitons. Consequently, relaxation of $^3\text{CT} \rightarrow T_1$ produces an irreversible loss of carriers. Surprisingly, even while energetically favored, the relaxation of triplet charge transfer (^{3}CT) states to lower lying triplet (T_1) excitons is *slower* in systems with a higher degree of molecular order at the heterojunction interface thereby allowing for the dissociation of ^{3}CT states back to free charges [14–16]. This effectively reduces loss due to recombination and enhances the overall performance of the device. [17]

A rationalization for this effect is that the ^{3}CT wave function is more delocalized in systems with higher degrees of ordering [14–18]. To explore this, we can write the coupling matrix element between an interfacial ^{3}CT and a triplet exciton localized in either the donor or acceptor phase as

$$V = \langle \psi_T | v(12) | \psi_{CT} \rangle. \quad (1)$$

Since we are concerned with triplet states involving single electron/hole excitations, we have only the "direct" coupling term between electron/hole configurations. In polymer/fullerene heterojunctions, the triplet exciton is generally localized in the polymer phase and we assume that this state is unaffected by molecular disorder in the fullerene phase. On the other hand, the ^{3}CT state will be sensitive to disorder in the fullerene phase. Increasing electronic localization to orbitals near the interface increases the overall coupling matrix element and the rate of relaxation from the higher-lying ^{3}CT to the lower lying triplet exciton states.

The inverse participation ratio (IPR) is a convenient estimate of the number of basis states populated by a given wave function

$$IPR = \frac{1}{\sum_i |\psi_n(i)|^4} \quad (2)$$

where $1 \leq IPR \leq N$ for normalized states ψ_n. In the limiting cases the wave function is either localized in a single basis state ($IPR = 1$) or delocalized uniformly over all N basis states ($IPR = N$). Thus, we can anticipate from these arguments that ^{3}CT states with higher IPR (i.e. more delocalized) are more weakly coupled to the triplet excitons than states with lower IPRs and increasing disorder in the fullerene phase would lead to an increase in the rate of relaxation from interfacial charge-transfer states into lower-lying molecular exciton states.

However, the local density of states (DOS) also contributes to the relaxation rate. If the DOS in the neighbourhood of the ^{3}CT is broadened by local energetic disorder and overlaps with the ^{3}CT density of states , initial population in ^{3}CT will rapidly decay into these nearby states having various degrees of mixing between purely excitonic and non-excitonic (charge-separated) electron/hole configurations. This will also lead to a rapid cascade of population from ^{3}CT to lower-lying charge-transfer excitons.

Bittner and Silva recently showed that delocalization of the *singlet* CT wave functions do effectively couple to asymptotic charge-separated states via phonon fluctuations. This previous work focused upon the initial dissociation of a singlet exciton state into a continuum of polaron states and explored the role of phonon fluctuation, quantum decoherence, and noise in driving charge-separation. [13] Here we the use a similar approach to analyze the recombination of triplet charge-transfer states by comparing relaxation rates of interfacially bound triplet charge-transfer states into triplet excitons in one and two dimensional models of a polymer/fullerene bulk-heterojunction with varying degrees of energetic disorder within the fullerene phase. These calculations allow us to study the effects of wave function delocalization, energetic disorder, dimensionality, and electronic mobility in a generic model with controllable parameters.

2 Theoretical Methods

We constructed a fully quantum-mechanical/finite temperature model for a polymer-fullerene heterojunction consist-

ing of parallel stacked polymers along a domain of acceptor (fullerene) sites. Each site contributes a valance and a conduction band Wannier orbital and the electronic ground state is where each valance orbital is doubly occupied. Each site also contributes two localized phonon modes which modulate the local energy gap at each site. Linear coupling between localized phonons give rise to optical phonon bands that are delocalized over each polymer chain. The electron/phonon couplings were determined by experimental Huang-Rhys factors for poly-pheneylene-vinylene type polymers. Single electron/hole excitations from the ground state are considered within configuration interaction (CI) theory.

We consider the electronic states and transitions between excitonic and polaronic states in a system of stacked polymer chains using a Hamitonian of the general form:[19–22].

$$\hat{H} = \hat{H}_{el} + \hat{H}_{ph} + \hat{H}_{el-ph}. \quad (3)$$

The electronic part $\hat{H}_{el}$ reflects the configuration interaction (CI) of single excitations for a generic two-band polymer in a localized basis. Each site within our model contributes a doubly occupied valance orbital and an unoccupied conduction orbital which can be loosely considered to be the local HOMO and LUMO orbitals of a singlet molecular subunit of our polymer chain. We consider here only single electron/hole excitations of the form

$$|n,\bar{m}\rangle = \frac{1}{\sqrt{2}}(a^{\dagger}_{n\uparrow}a_{\bar{m}\uparrow} + a^{\dagger}_{n\downarrow}a_{\bar{m}\downarrow})|0\rangle$$

where $a_{\bar{m}\sigma}$ removes an electron with spin σ from an occupied valance orbital (or HOMO) on site m (creating a hole) and $a^{\dagger}_{n\sigma}$ places it in the unfilled conduction orbital (or LUMO) of site n. The configurations $|\mathbf{m}\rangle = |\overline{m}m\rangle$ taken over valence and conduction-band Wannier functions $|\overline{m}\rangle$ and $|m\rangle$ represent all geminate ($\overline{m} = m$) and charge-transfer ($\overline{m} \neq m$) e-h pairs for the model lattice.

The electron-phonon coupling term $\hat{H}_{el-ph}$ assumes that the localized conduction/valence levels and nearest-neighbor transfer integrals are modulated by linear coupling to the phonons. Correspondingly, the phonon term consists of two sets of interacting local oscillators, giving rise to two dispersed optical phonon branches centered at 1600 and 100 cm^{-1}, respectively. These frequencies correspond to the C=C bond stretches and ring torsions in PPV both of which dominate the Franck-Condon activity of the lowest optical transitions. By empirical adjustment of electron-phonon coupling strength in $\hat{H}_{el-ph}$, we can compute within the Condon approximation accurate absorption and emission band-shapes for PPV chains, reflecting conjugation-length dependence, vibronic structure, and Stokes shifts.[20] For the sake of constructing a model, we assume these parameters are transferrable to the generic class of organic semiconducting materials.

Diagonalizing $\hat{H}_{el}$ and $\hat{H}_{ph}$ yields a variety of vertical excited states with energies ε^{o}_{a} and normal modes with frequencies ω_{ξ}, which allow us to transform the electron-phonon coupling term within the diabatic representation.

$$\begin{aligned}\hat{H} &= \sum_{a}\varepsilon^{o}_{a}|\mathbf{a}\rangle\langle\mathbf{a}| + \frac{1}{2}\sum_{\xi}\left(\omega^{2}_{\xi}Q^{2}_{\xi} + P^{2}_{\xi}\right) \\ &+ \sum_{ab\xi} g^{o}_{ab\xi}Q_{\xi}|\mathbf{a}\rangle\langle\mathbf{b}|. \end{aligned} \quad (4)$$

With the exception of the energy off-sets and interchain hopping terms, a complete listing of the electron/hole interaction terms and parameters is given in Ref. 20.

The manifold of electronic states produced by a given model will contain a wide spectrum of states with various degrees of mixing between purely charge-transfer and purely excitonic electron/hole configurations. Within the density of states, we define the interfacial charge transfer (CT) state as the lowest energy state in which the hole is localized to the greatest extent on the interfacial donor orbitals and the transferred electron is localized to the greatest extent on the interfacial acceptor orbitals. Once we have identified the triplet CT state, we compute the rate for population to decay from the CT state into all other states using the Fermi's golden rule expression

$$k_{ab} = \pi\omega^{2}_{ab}(n(\omega_{ab})+1)(J(+\omega_{ab}) - J(-\omega_{ab}))$$

where $n(\omega)$ is the Bose-Einstein distribution and $J(\omega)$ is the spectral density of the phonon bath evaluated at the electronic transition frequency,

$$J(\omega) = \sum_{q} g^{2}_{abq}\delta(\omega - \omega_{q}),$$

and at $T = 300K$. As input, the electron-phonon couplings g_{abq}, phonon frequencies, ω_{q}, and electronic transition frequencies, ω_{ab} are obtained by diagonalizing the electronic Hamiltonian for our model[23–26]. Lastly, we compute a reduced IPR for the charge transferred to the acceptor orbitals by defining

$$IPR = \frac{1}{\sum_{i}|p_{e}(i)|^{2}} \quad (5)$$

where $p_{e}(i)$ is the occupation of the ith conduction band orbital for each initial ^{3}CT state. This gives a quantitative measure of the delocalization of the negative charge in the initial state. Random sampling over the acceptor site energies gives an average measure of the localization of the charge transferred to the acceptor phase versus disorder.

We have used this approach previously to describe the energetics, dynamics, and spectroscopy of polymer-based donor-acceptor systems and diodes[19,22,27] More recently, we have

used this approach, combined with a non-Markovian master equation technique[28,29] to understand ultrafast singlet exciton fission in terms of direct tunneling to polaron bands.[13] The model can provide the necessary input for describing the dynamics of a polymer-based photovoltaic cell[28,30,31]. A lattice model for a bulk-heterojunction was presented recently by Troisi that includes many of the features of our model, but does not include explicit phonons and electronic transitions between states are introduced via the semiclassical Marcus theory[32].

3 Model Heterojunction Systems

We now apply our model to a series of prototypical models for a bulk-heterojunction system. This allows us to consider the effects of dimensionality, local electronic coupling, and local energy disorder on the electronic states, their couplings, and interstate relaxation rates as we vary one or more key parameters. If wave function delocalization is the determining factor in suppressing triplet charge recombination in polymer/fullerene based heterojunction systems as suggested by recent experiments by Bernardo et al.[15] and Rao *et al.*[14], we anticipate that the relaxation rate from an initially prepared interfacial triplet CT to lower-lying triplet excitons should increase with increasing energetic disorder and correspondingly decrease with increasing electronic delocalization in the acceptor phase.

3.1 One dimensional, colinear chain model

We first consider a quasi-one dimensional chain partitioned into donor and acceptor domains, each with 10 sites respectively. We introduce "energetic disorder" into our model by sampling the energies for the acceptor orbitals from a normal distribution about their mean value with variance δE^2. This is to account for any structural or other inhomogeneous broadening of the local electronic energies within the acceptor phase. By increasing δE, the electronic states in the acceptor phase become increasingly localized.

In Fig. 2 we show the probability distribution function (PDF) of relaxation rates from the ^{3}CT state as δE increases from 0 to 0.1 in units of the electronic hopping term between neighboring sites, $t_{\|}$. Increasing δE broadens and skews the distribution of rates towards faster decay rates. In the inset of Fig. 2 we compare the average decay rate $\langle k \rangle$ and the IPR for the valence-band electron in the initial ^{3}CT state. The average shows a systematic increase with increasing δE. Also shown in the inset is the average IPR for the electron density in the conduction orbitals. In the absence of disorder in the site energies, the conduction-band electron is delocalized over more than 7 lattice sites. Upon increasing the energy variance

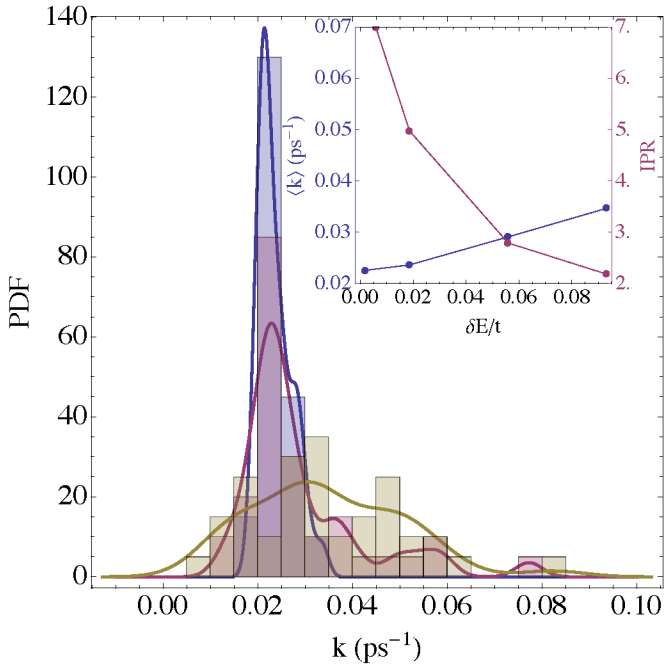

Fig. 2 Distribution of ^{3}CT relaxation rates for the 1D-colinear chain model. Colored curves and bars correspond to increasing degrees of energetic disorder. Blue: $\delta E/t_{\|} = 0.018$, Red: $\delta E/t_{\|} = 0.056$, Gold: $\delta E/t_{\|} = 0.093$, Inset: Average ^{3}CT relaxation rates vs. variance in site energy (blue curve/left-axis); Average IPR for the valence electron in the initial ^{3}CT state (red curve/right-axis).

to $\delta E/t = 0.1$ localizes the conduction electron in the triplet CT state to the 2 sites closest to the interface.

The one-dimensional model is entirely consistent with the idea that increases in the decay rate k reflect increasing localization of the CT wave function to sites nearest the interface and provides a rationalization for the trends observed in Ref. 14. However, the density of states is highly sensitive to dimensionality and a one-dimensional model may not properly capture the full physics in this system. With this in mind, we consider a series of lattice models designed to capture the effects of π-stacking and increased dimensionality to test whether or not wave-function localization correlates with an increase in the ^{3}CT $\rightarrow$ T$_1$ relaxation kinetics in general.

3.2 Parallel chains with energy disorder

We next consider two parallel cofacial polymer chains defining separate donor and acceptor molecules, each with 10 sites. A segment of the model is sketched below where thick black lines denote π-bonding between sites and thin lined denote weaker π-stacking or intermolecular interactions.

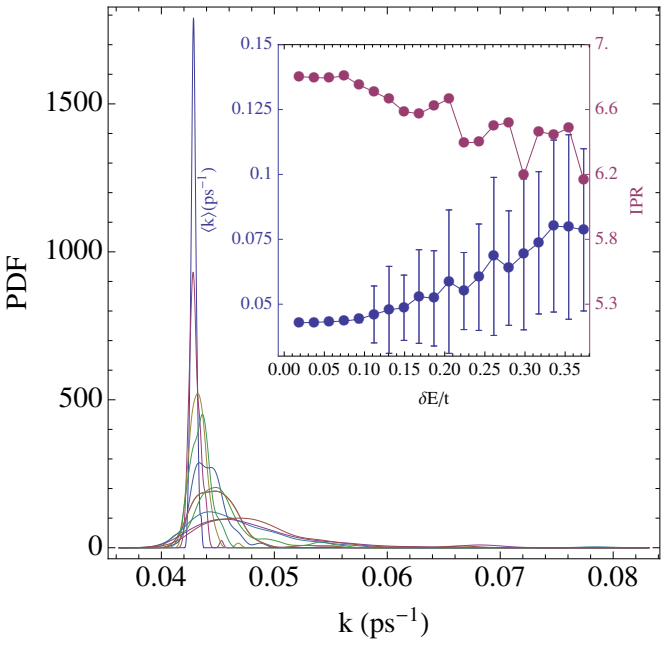

Fig. 3 Distribution of ^{3}CT relaxation rates for the cofacial polymer chain model. Colored curves and bars correspond to increasing degrees of energetic disorder. Average IPR for the valence electron in the initial ^{3}CT state (red curve/right-axis).

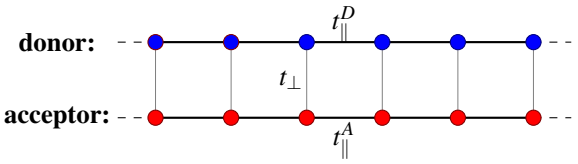

We randomize the orbital energies only on the acceptor side and take the interchain electronic hopping term ($t_\perp$) to be an order of magnitude smaller than the intrachain hopping term $t_\parallel^A = t_\parallel^D = t = 10t_\perp$. In this case, the hole remaining on the donor can propagate freely along the chain while the transferred charge will experience a disordered energy landscape along the polymer backbone.

In Fig. 3 we show the distribution of relaxation rates from an initially prepared triplet inter-chain CT state as well as the average rate and IPR with increasing levels of disorder in the acceptor site energies. In comparison to the linear model, the average IPR for the ^{3}CT shows little variation with increasing $\delta E/t$, decreasing from 6.6 to 6.2. This is understandable since the Coulomb attraction between the electron and hole is much stronger than the energetic disorder on the acceptor side. In other words, the electron is pulled over a rough energy landscape by a hole moving freely along the polymer backbone. The ^{3}CT relaxation rates systematically broaden as the energetic disorder increases and the tail towards higher rates causes the mean rate to shift towards faster rates.

3.3 Parallel chains without energy disorder

We next consider the case of four parallel (co-facial) chains, two in each of the donor and acceptor phases respectively. For the donor side, we take the interchain hopping integral to be constant $t_{DA} = 0.1t_\parallel$ and systematically vary the interchain integral on the acceptor side, $t_\perp^A$ from 0 to 0.5 $t_\parallel$. Physically, this corresponds to increasing the mobility of the electron in the donor phase in the direction perpendicular to the interface and very large values of $t_\perp^A$ would correspond to an extension of the π-bonding network between the two chains. A sketch of this model is shown here.

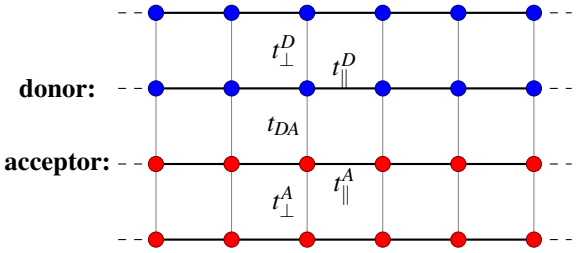

In Fig. 4a we plot the ^{3}CT relaxation rates, IPR, and nearby eigenstate energies versus the ratio of the interchain vs. intrachain hopping integrals, $r = t_\perp^A/t_\parallel$. As one expects, increasing r increases the delocalization of the electronic states within the acceptor domain and corresponds to an increase in charge mobility. However, increasing r also lowers the energy levels for the electronic states localized in the acceptor phase without affecting to a great extent the states localized in the donor phase. The sharp rise and fall of the ^{3}CT relaxation rate (Fig. 4a) corresponds to the avoided crossing shown in Fig. 4b at $r = 0.3$ between the interfacial ^{3}CT and nearby triplet excitonic states localized within the donor phase. If we take the lower range of r to be representative of physical systems involving polymers and fullerenes, increasing the perpendicular electronic coupling in the acceptor phase would lead to an overall *increase* in the triplet CT relaxation rate for a 2D polycrystalline system. These results are very sensitive to the parameterization of the model over a broad-range of r and realistically, one should consider only the regime where $r \approx 0.1$. However, even over the limited range, this trend is contrary to the experimental results in which the triplet CT relaxation rate decreases with increasing perpendicular electron mobility in the fullerene phase.

3.4 Two dimensional-bulk heterojunction model

Lastly, we consider a model more akin to a polymer/fullerene bulk heterojunction (BHJ). The 2D-BHJ model consists of four parallel polymer chains in the donor phase abutting a simple square lattice of fullerene (electron acceptor) sites as sketched below.

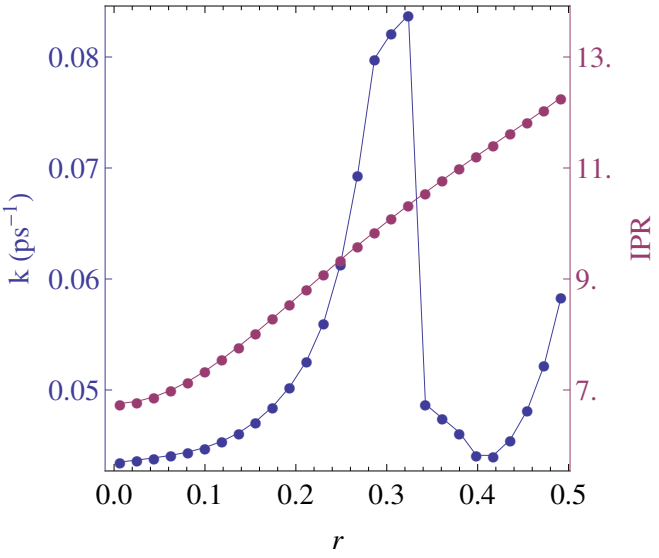

(a)

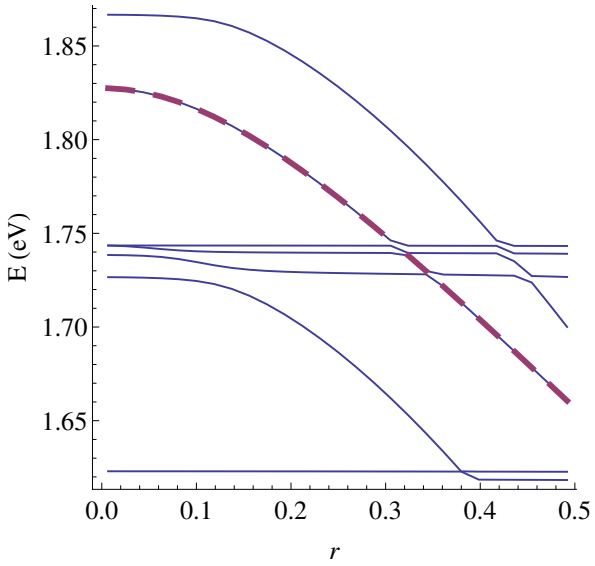

(b)

Fig. 4 (a) ^{3}CT relaxation rates (red) and IPR (blue) (b) eigenstate energies vs. coupling strength vs. $r = t_\perp^A/t_\parallel^A$ for the parallel polymer chains (model C). Here, the increase and decrease in relaxation rate from the initially populated triplet CT state with increasing interchain coupling correlates with an avoided crossing between nearby states. The thick-dashed line in (b) identifies the interfacial ^{3}CT state.

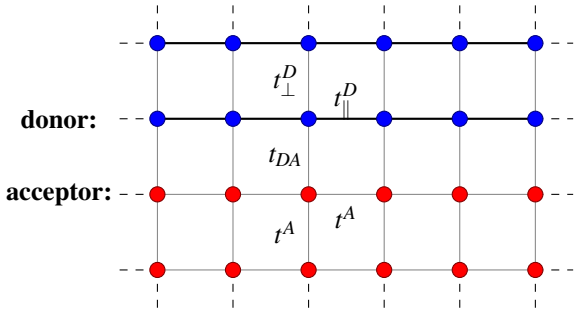

Energetic disorder is introduced only into the fullerene (acceptor) site energies and we set the t^A hopping integral between fullerenes to be the same as the $t_{DA} = t_\perp^D$ interchain hopping term between polymer sites, which we approximate as $t_\parallel^D/10$.

In Fig. 5 we compare the density of triplet states in the neighbourhood of the ^{3}CT with increasing amounts of energy disorder in site energies. At the low end of the DOS, at $\approx$ 2.1eV, are bands of triplet excitons. These states consist entirely of geminate electron/hole configurations entirely within the polymer side of the system. Between 2.2 and 2.5 eV is a band of excitons that lie entirely on the fullerene side of the junction. These are composed of geminate (excitonic) electron/hole configurations that are predominantly localized to single fullerene units. The interfacial ^{3}CT states lie in the valley at 2.7 eV between the fullerene triplets and the broad continuum corresponding to states with various admixtures of excitonic and charge-separated character including free polarons.

In the absence of energetic disorder, the 2D-BHJ model produces a singlet (S_1) exciton energy of 2.6 eV and a singlet charge transfer state ^{1}CT at 2.4 eV. For the triplet states, the T_1 exciton is lowest in energy (1.2 eV) and is localized on one of the polymer chains. The triplet charge transfer states (^{3}CT) lie much higher in energy at 2.7eV. These states are embedded between a broad density of fullerene triplets and a continuum of charge-separated (CS) states. We distinguish between CT and CS states by whether or not the charge separation is between donor and acceptor sites at the interface (CT) or if the charges are separated by one or more sites away from the interface. Finally, we introduce "disorder" into our model by sampling the valance and conduction site energies for the fullerene sites from a normal distribution about a mean value with variance δE^2. This is to account for any structural or other inhomogeneous broadening of the local fullerene electronic energies. Increasing δE, the electronic states in the fullerene phase become increasingly localized.

Generally speaking, one expects that triplet states lie lower in energy than their corresponding singlets. This arises from the fact that the electron/hole interaction for triplets is simply the Coulomb interaction whereas for singlets, the electron/hole interactions include both Coulomb and exchange contributions. Both J and K are positive-definite contributions

that can be parameterized in terms of the separation distance between the electron and hole, r_{eh}. For a given electron/hole configuration: $V_T = -J(r_{eh})$ while $V_S = -J(r_{eh}) + 2K(r_{eh})$. Consequently, the difference between equivalent singlet and triplet states is $E_S - E_T \approx 2K$. This is certainly the case in comparing the triplet and singlet exciton states produced by our heterojunction model. In all cases, the lowest lying singlet exciton ^{1}S, as determined by the CI eigenstate with the largest oscillator strength to the ground electronic state, is higher in energy (2.6eV) than the lowest energy triplet excitonic state.

However, this simple rule is more difficult to apply when comparing the ^{1}CT and ^{3}CT energies. For the 2D-BHJ model, the lowest energy singlet at 2.4 eV is a charge transfer state pinned to sites at the interface. The equivalent ^{3}CT lies higher in energy at 2.7eV and is embedded above a broad density of states corresponding to triplet excitons localized in either the donor or acceptor phase. Closer inspection of the ^{3}CT indicates mixing between charge-transfer configurations and purely excitonic configurations whereas the ^{1}CT is purely charge-transfer in character. Mixing between charge-transfer and purely excitonic configurations destabilizes the ^{3}CT.

Increasing energetic disorder broadens the DOS of the fullerene triplet excitons. Since the ^{3}CT spans both polymeric and fullerene sites, the ^{3}CT energy is also inhomogeneously broadened upon sampling over multiple realizations of the model. Importantly, with increasing energy disorder, an increasing number of states with exciton/charge-separated character begin to appear in the vicinity of the ^{3}CT state.

In Fig. 6 we show the distribution of relaxation rates from the ^{3}CT for various degrees of energetic disorder. As in the 1D case, the distribution is peaked around $k = 0.03\text{ps}^{-1}$ and becomes highly skewed towards higher rates as energetic disorder is increased. The inset of Fig. 6 shows both the mode and median of the distribution. The peak (mode) of the distribution shows very little variation with increasing energetic disorder. However, once the disorder in the site energies is on the order of the inter-unit hopping term $\delta E/t > 1$ the median and mode diverge. In comparison, the IPR for the conduction-band electron in the initial ^{3}CT (inset of Fig. 6) shows little systematic variance as $\delta E/t$ is increased. This can be understood in light of the fact that the single-particle hopping term within the fullerene phase is small compared to the Coulomb integral for the ^{3}CT state. As a result the ^{3}CT state is pinned within the first row of fullerene sites at the interface and does not extend deeply into the bulk.

Closer examination of the population relaxation dynamics for the specific cases giving rise to the tail in Fig. 6 reveals that as energetic disorder is increased, there is a increasing density of states in the vicinity of the initial ^{3}CT composed both charge-separated (CS) electron/hole configurations and excitonic configurations within the polymer phase. These states may serve as intermediate "gateways" into the manifold of lower polymer triplet excitons, giving rise to a broad-range of relaxation timescales. Furthermore, mixing between the ^{3}CT and fullerene triplets may also explain the intense fullerene phosphorescence reported by Schlenker *et al.* in polymer/fullerene based devices[33].

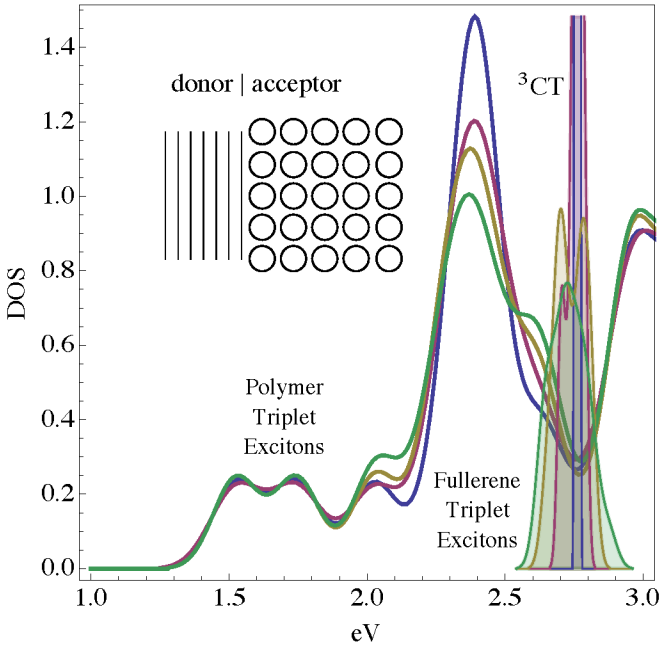

Fig. 5 Density of triplet states in the neighbourhood of the ^{3}CT for 2D-BHJ model. Colored curves indicate various degrees of energetic disorder. Blue: $\delta E/t_\perp = 0.25$, Red: $\delta E/t_\perp = 1$, Gold: $\delta E/t_\perp = 1.4$, Green: $\delta E/t_\perp = 2$. (Inset) Sketch of the 2D heterojunction model.

4 Discussion

We have presented a series of model heterojunction systems to explore the role of wave function localization in the irreversible relaxation of a triplet ^{3}CT state into triplet excitons. In Ref. 14, triplet formation is observed in BHJ devices made with ICBA and ICMA blends with PIDT-PhanQ but not observed in PIDT-PhanQ:PCBM blends. It is known that PCBM effectively forms large aggregates and that aggregation facilitates charge-separation.[16] The supposition is that in the more crystalline materials, the CT state is delocalized over more fullerenes and that this facilitates the initial charge separation *and* suppresses bimolecular recombination of triplet polaron pairs. Within the context of our theoretical model, the relaxation rate from an initially prepared interfacial triplet CT to lower-lying triplet excitons should increase with increasing energetic disorder and correspondingly decrease with increasing electronic mobility in the acceptor phase.

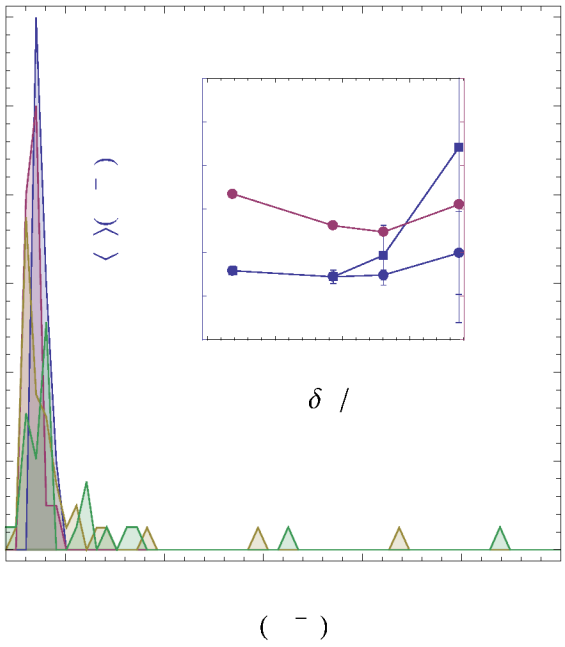

Fig. 6 Distribution of ^{3}CT relaxation rates for the 2D-BHJ model. Colored curves indicate various degrees of energetic disorder. Blue: $\delta E/t_\perp = 0.25$, Red: $\delta E/t_\perp = 1$, Gold: $\delta E/t_\perp = 1.4$, Green: $\delta E/t_\perp = 2$. Inset: Average ^{3}CT relaxation rates vs. variance in site energy (blue curve/left-axis); Average IPR for the valence electron in the initial ^{3}CT state (red curve/right-axis).

The 1D co-linear and cofacial models do support the delocalization hypothesis. For a given interchain coupling within the acceptor phase, increasing energetic disorder (which implies decreasing mobility) both localizes the ^{3}CT wave function and leads to an increase in the average relaxation rate. However, in parallel chains without energetic disorder–which should correspond to the purely crystalline limit– increasing the inter-layer mobility ($t_\perp^A$) increases the delocalization of the ^{3}CT wave function and over a suitable parametric range of the mobility. However, the ^{3}CT relaxation rate also *increases*, contrary to our original supposition.

In the 2D-BHJ model, increasing the energetic disorder within the fullerene phase has a small effect on the average localization of the initial ^{3}CT wave function and the most-likely rate (*i.e.* the mode) shows very little variation with increasing energetic disorder. Even in the limit with no energetic disorder, the transferred electron is shared amongst at most 3 acceptor sites at the interface and does not extend deeply into the bulk of the acceptor phase. Introducing energetic disorder in to the fullerene phase produces a distribution of ^{3}CT relaxation rates with a tail that increasingly extends towards faster rates with increasing disorder, resulting in a faster averaged relaxation rate upon summing over configurations.

The interplay between dynamics, state-localization, and dimensionally can be very subtle. What is clear from these studies is that energetic order in the vicinity of the interface plays a central role in determining the emergent behavior of a BHJ device. Further experimental and theoretical work is necessary to refine our understanding of these effects and gain control of how material properties influences quantum states at the phase boundary between donor and acceptor materials. Recent work by Asbury's group reports that domain compositions and fullerene aggregation can strongly modulate charge photogeneration at ultrafast timescales. in high-performance polymer/fullerene devices.[34] The work supports the notion that higher polaron yields correlate with higher degrees of order in the fullerene domain.

Acknowledgments The work at the University of Houston was funded in part by the National Science Foundation (CHE-1362006) and the Robert A. Welch Foundation (E-1334). D.S.G. acknowledges support from ONR under award N00014-14-1-0170.

References

1 Z. He, C. Zhong, S. Su, M. Xu, H. Wu and Y. Cao, *Nature Photonics*, 2012, **6**, 591–595.
2 B. H. Wallikewitz, D. Kabra, S. Gélinas and R. H. Friend, *Phys. Rev. B*, 2012, **85**, 045209.
3 N. Sariciftci and A. Heeger, *International Journal of Modern Physics B*, 1994, **8**, 237–274.
4 N. Banerji, S. Cowan, M. Leclerc, E. Vauthey and A. J. Heeger, *Journal of the American Chemical Society*, 2010, **132**, 17459–17470.
5 M. Tong, N. Coates, D. Moses, A. J. Heeger, S. Beaupré and M. Leclerc, *Phys. Rev. B*, 2010, **81**, 125210.
6 C.-X. Sheng, T. Basel, B. Pandit and Z. V. Vardeny, *Organic Electronics*, 2012, **13**, 1031–1037.
7 A. E. Jailaubekov, A. P. Willard, J. R. Tritsch, W.-L. Chan, N. Sai, R. Gearba, L. G. Kaake, K. J. Williams, K. Leung, P. J. Rossky and X.-Y. Zhu, *Nat Mater*, 2013, **12**, 66–73.
8 G. Grancini, M. Maiuri, D. Fazzi, A. Petrozza, H.-J. Egelhaaf, D. Brida, G. Cerullo and G. Lanzani, *Nat Mater*, 2013, **12**, 29–33.
9 L. G. Kaake, D. Moses and A. J. Heeger, *The Journal of Physical Chemistry Letters*, 2013, 2264–2268.
10 N. Banerji, *J. Mater. Chem. C*, 2013, **1**, 3052.
11 S. Gélinas, A. Rao, A. Kumar, S. L. Smith, A. W. Chin, J. Clark, T. S. van der Poll, G. C. Bazan and R. H. Friend, *Science*, 2013, **343**, 521–516.
12 F. Provencher, N. Bérubé, A. W. Parker, G. M. Greetham, M. Towrie, C. Hellmann, M. Côté, N. Stingelin, C. Silva and S. C. Hayes, *Nat Mater*, 2014, **in press**, year.
13 E. R. Bittner and C. Silva, *Nat Commun*, 2014, **5**, 3119.
14 A. Rao, P. C. Y. Chow, S. Gelinas, C. W. Schlenker, C.-Z. Li, H.-L. Yip, A. K. Y. Jen, D. S. Ginger and R. H. Friend, *Nature*, 2013, **500**, 435–439.
15 B. Bernardo, D. Cheyns, B. Verreet, R. D. Schaller, B. P. Rand and N. C. Giebink, *Nat Commun*, 2014, **5**, 3245.
16 F. C. Jamieson, E. B. Domingo, T. McCarthy-Ward, M. Heeney, N. Stingelin and J. R. Durrant, *Chem. Sci.*, 2012, **3**, 485–492.
17 P. C. Y. Chow, S. Gélinas, A. Rao and R. H. Friend, *Journal of the American Chemical Society*, 0, **0**, null.
18 A. A. Bakulin, A. Rao, V. G. Pavelyev, P. H. M. van Loosdrecht, M. S. Pshenichnikov, D. Niedzialek, J. Cornil, D. Beljonne and R. H. Friend, *Science*, 2012, **335**, 1340–1344.

19 S. Karabunarliev and E. R. Bittner, *The Journal of Chemical Physics*, 2003, **119**, 3988–3995.

20 S. Karabunarliev and E. R. Bittner, *The Journal of Chemical Physics*, 2003, **118**, 4291–4296.

21 S. Karabunarliev and E. R. Bittner, *Journal of Physical Chemistry B*, 2004, **108**, 10219–10225.

22 S. Karabunarliev and E. R. Bittner, *Physical Review Letters*, 2003, **90**, 057402.

23 E. R. Bittner and S. Karabunarliev, *International Journal of Quantum Chemistry*, 2003, **95**, 521–531.

24 S. Karabunarliev and E. R. Bittner, *Physical Review Letters*, 2003, **90**, APS.

25 S. Karabunarliev and E. R. Bittner, *The Journal of Chemical Physics*, 2003, **119**, AIP–3995.

26 V. May and O. Kühn, *Charge and Energy Transfer Dynamics in Molecular Systems*, Wiley-VCH, 2nd edn, 2004.

27 E. R. Bittner, J. G. S. Ramon and S. Karabunarliev, *The Journal of Chemical Physics*, 2005, **122**, 214719–9.

28 A. Pereverzev and E. R. Bittner, *The Journal of Chemical Physics*, 2006, **125**, 104906.

29 A. Pereverzev, E. R. Bittner and I. Burghardt, *The Journal of Chemical Physics*, 2009, **131**, 034104.

30 H. Tamura, E. R. Bittner and I. Burghardt, *The Journal of Chemical Physics*, 2007, **126**, 021103.

31 H. Tamura, J. G. S. Ramon, E. R. Bittner and I. Burghardt, *Physical Review Letters*, 2008, **100**, 107402.

32 A. Troisi, *Faraday Discussions*, 2013.

33 C. W. Schlenker, K.-S. Chen, H.-L. Yip, C.-Z. Li, L. R. Bradshaw, S. T. Ochsenbein, F. Ding, X. S. Li, D. R. Gamelin, A. K.-Y. Jen and D. S. Ginger, *Journal of the American Chemical Society*, 2012, **134**, 19661–19668.

34 S. V. Kesava, Z. Fei, A. D. Rimshaw, C. Wang, A. Hexemer, J. B. Asbury, M. Heeney and E. D. Gomez, *Advanced Energy Materials*, 2014, **4**, 1400116.